Meteorologische Zeitschrift, Vol. **26**, No. 3, 307–317 (published online March 10, 2017)

Hourly weather forecasts for gas turbine power generation

G. Giunta[1], R. Vernazza[1], R. Salerno[2], A. Ceppi[3*], G. Ercolani[3,4] and M. Mancini[3]

[1]Eni S.p.A., Development Operations & Technology, San Donato Milanese, Italy
[2]Epson Meteo Centre, Sesto S. Giovanni, Italy
[3]Department of Civil and Environmental Engineering, Politecnico di Milano, Milan, Italy
[4]Present affiliation: Department of Civil and Environmental Engineering, University of Florence, Florence, Italy

(Manuscript received March 9, 2016; in revised form December 15, 2016; accepted December 20, 2016)

Abstract

An hourly short-term weather forecast can optimize processes in Combined Cycle Gas Turbine (CCGT) plants by helping to reduce imbalance charges on the national power grid. Consequently, a reliable meteorological prediction for a given power plant is crucial for obtaining competitive prices for the electric market, better planning and stock management, sales and supplies of energy sources. The paper discusses the short-term hourly temperature forecasts, at lead time day+1 and day+2, over a period of thirteen months in 2012 and 2013 for six Italian CCGT power plants of 390 MW each (260 MW from the gas turbine and 130 MW from the steam turbine). These CCGT plants are placed in three different Italian climate areas: the Po Valley, the Adriatic coast, and the North Tyrrhenian coast. The meteorological model applied in this study is the eni-Kassandra Meteo Forecast (e-kmf™), a multi-model approach system to provide probabilistic forecasts with a Kalman filter used to improve accuracy of local temperature predictions. Performance skill scores, computed by the output data of the meteorological model, are compared with local observations, and used to evaluate forecast reliability. In the study, the approach has shown good overall scores encompassing more than 50,000 hourly temperature values. Some differences from one site to another, due to local meteorological phenomena, can affect the short-term forecast performance, with consequent impacts on gas-to-power production and related negative imbalances. For operational application of the methodology in CCGT power plant, the benefits and limits have been successfully identified.

Keywords: air temperature forecast, weather model performance, power output, gas-to-power generation, CCGT power plant

1 Introduction

Recent years have witnessed significant efforts worldwide, from research to policy initiatives, to support the interaction of various energy vectors (e.g. natural gas and electricity), and sectors at different levels (e.g. from demand to generation), in a smart grid integration scenario (Crisostomi et al., 2013). The paper analyzes the impact of weather variability in this profound reassessment of the energy infrastructure, and the importance of a reliable meteorological forecast.

It is well known that power generation from wind and solar plants is strongly dependent on weather. Then, following a policy of smart grid integration, the power balance is guaranteed by other sources, such as Combined Cycle Gas Turbine (CCGT) plants for power and steam generation (Kehlhofer et al., 2009; Rovira et al., 2011). They have become common in several countries around the world even in those with large variability of climatic conditions, which strongly affects the performance of gas turbines particularly in warm seasons, when demands for electricity are generally higher. Despite their numerous applications, one of the most important shortcomings affecting Gas Turbine (GT) process behavior is that their power output decrease at high air temperatures during very hot and humid summers (De Felice et al., 2015; Farouk et al., 2013). By cooling the air down at the gas turbine intake, the power output penalties can be mitigated by using an air-cooling method: i.e. evaporative cooling, refrigeration cooling (Kakaras et al., 2005). These climate conditions affect air density, which flows through the compressor, reducing power output of the gas turbine of about 2 MW for 1 Celsius degree. Currently, CCGT plants use various techniques to cool inlet air and boost turbine output, including evaporative coolers and mechanical chillers (Boonnasa, 2006; Zadpoor and Golshan, 2006), that entail additional energy consumption and power output reduction.

In this framework, temperature forecasts play a strategic role permitting to achieve the maximum power output at the most convenient time with respect to the market request in terms of both grid balance and maximization of incomes. For optimization strategy, weather variables (i.e. air temperature, relative humidity, pressure) and economic parameters (i.e. electrical demand, electricity tariff, and gas prices) have to be simultaneously considered (Gareta et al., 2004).

*Corresponding author: Alessandro Ceppi, Department of Civil and Environmental Engineering, Politecnico di Milano, Piazza Leonardo da Vinci 32, 20133 Milano, Italy, e-mail: alessandro.ceppi@polimi.it

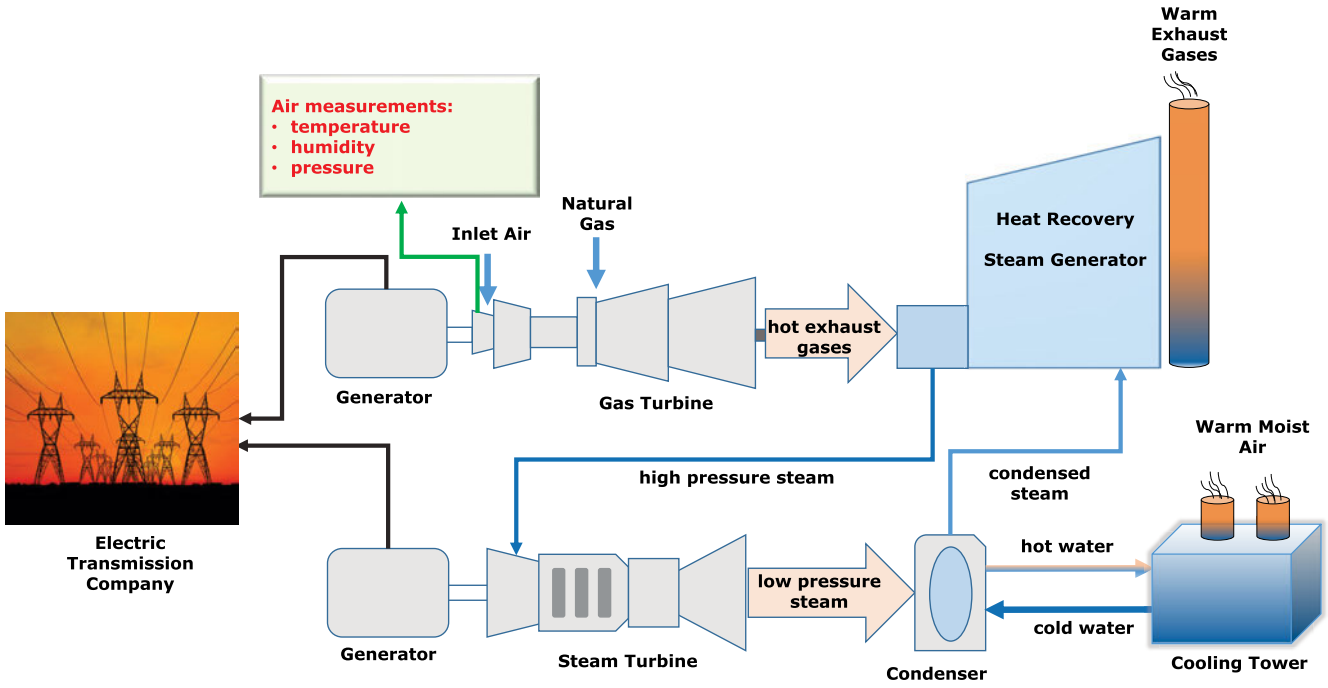

Figure 1: CCGT plant scheme fitted with local meteorological data measurements placed near the air inlet.

An accurate weather forecast provided by a high resolution Limited Area Model (LAM), can be used for optimizing the power generation process in CCGT plants, reducing the penalties related to imbalance charges on the national power grid and obtaining competitive prices in the national energy market (Giunta and Salerno, 2013).

The present paper focuses on the application of short-term temperature forecasts and their sensitivity to specific errors which may have impacts on energy predictions for power plants. Forecast analysis has been performed on six Enipower CCGT plants of 390 MW power each (placed to Mantova, Brindisi, Livorno, Ravenna, Ferrara, and Ferrera Erbognone), in particular 260 MW from the gas turbine and 130 MW from the steam turbine, and it has been carried out over thirteen months, from 1 August 2012 to 31 August 2013. This work analyses the different phenomena among climate areas and the model capability to forecast temperatures, taking into account the meteorological episodes occurring in each location. Performance skill scores have been used to understand the reliability of hourly temperature forecasts provided by the meteorological model e-kmf™ (eni–Kassandra Meteo Forecast) at lead time day+1 and day+2. The metrics for temperature forecast evaluation includes standard statistical indexes commonly used in scientific literature, computed on the output of the meteorological model compared with observed data in each plant. The obtained results point out the performances of the e-kmf™ model on a forecast horizon of 48 hours, which is the target in the gas-to-power production planning, the forecast errors occurring during significant changes of weather conditions (i.e. variations in daily temperatures higher than ±4 K in two consecutive days), and local scale phenomena such as fog, thunderstorms and orographic winds.

The paper is organized as follows: Section 2 consists in a description of the weather model used, and some climatological hints over the CCGT plant areas; Section 3 describes the main achievements of the e-kmf™ hourly forecasts with some remarks that should be required in its operational use, Section 4 discusses the impact of forecast temperature on power planning with consequent imbalances of power output.

2 Use of the meteorological model for temperature forecast in CCGT plant

The performance of Combined Cycle Gas Turbine (CCGT) power plants is significantly influenced by weather variables by considering the scheme of the GT module (Fig. 1). In fact, one of the main components of a gas turbine is the air compressor that, depending on density and composition of the fluid passing through it, varies its performance significantly. In particular, the most impacting element is the air inlet temperature, which should be the focus of attention on weather forecasting activities. The air temperature is, in fact, continuously measured by a passive shielded thermometer with ±0.1 K accuracy at 10 m from ground level, purposely where the air inlet is located, in order to obtain data as reliable as possible, since they are used for the regulation of natural gas combustion process.

In this framework, the role of a meteorological LAM is to support short-term energy production planning of CCGT power plant and to provide local temperature forecasts to be used as input variables in the producible

electrical energy algorithm. Hence, an accurate forecast of electrical energy production plays a relevant role, since temperature errors may have a significant impact. In fact, an over-planning (i.e. providing more energy than the combined cycle can deliver) may force the plant to pay negative imbalance charges; while, under-planning would not allow the exploitation of the production unit potentials.

2.1 The meteorological model for short-term forecast

Short-term forecast accuracy has improved as increasing computational power has allowed the use of progressively finer resolution, more sophisticated model physics, and better data assimilation procedures. However, inherent limits in atmospheric predictability (Lorenz, 1963; Lorenz, 1965; Lorenz, 1982), may reduce the value of further decreasing grid spacing in numerical weather prediction models (Mass et al., 2002). Moreover, numerical model forecasts can be very sensitive to slight changes in the larger-scale initial conditions. Recognition of such predictability issues has led to an increased interest in developing a different approach for further improving numerical weather forecasts, namely ensemble forecasting. Ensemble forecasting provides a useful way of addressing variability in the initial conditions, uncertainties in model physics, and the inherent uncertainty in atmospheric prediction. An approximation to the forecast Probability Density Function (PDF) of model variables can be defined by the calibrated frequency distribution of the resulting ensemble forecasts (Toth et al., 2001). Ensemble forecasts can provide additional value over deterministic forecasts, even if the initial and forecast PDFs are poorly defined. On average, the ensemble mean forecast tends to be a better estimate of the verifying state than each of the individual forecasts composing the ensemble. Hence, a combined multi-model, multi-analysis technique has been used in the e-kmf™ forecast system (Giunta et al., 2015). In this system, Ensemble Mean Forecast (EMF), which, hence, comprised forecasts from multiple modelling sources (i.e. varying physics) and using perturbed initial conditions, has displayed the lowest error scores. In several months of simulations, the EMF has shown lower 2 m temperature errors than the component members of the ensemble. Furthermore, EMF has been verified as the best forecast with about the same frequency as each component forecast; at the same time, it has never been verified as the worst forecast. Although this approach does not fit within the classic Monte Carlo method of generating perturbations to initial conditions, this system can represent an effective attempt to simulate the atmospheric evolution and may provide insights into the range of uncertainties which can be found in both the initial conditions and models. Multi-model approaches, which use a single analysis, attempt to overcome modelling system deficiencies, while multiple analyses with a single modelling system may diagnose sensitivity to the initial conditions. The combination of these two approaches can maximize the benefits of each one by compensating for deficiencies in both the initial conditions and the modelling systems.

The e-kmf™ consists of multi-component ensembles: the global ensemble provides lateral boundary conditions to a regional ensemble which provides the boundary conditions to a limited area. The global ensemble calculates the initial condition perturbations using the Ensemble Transform Kalman Filter (ETKF, Bishop et al., 2001). In this set-up, the regional ensemble provides the downscaling of the global ensemble; the local ensemble, in turn, provides the dynamical downscaling of the regional ensemble. Each higher resolution model provides the opportunity for small-scale features to grow in the ensemble. The regional ensemble uses interpolated perturbations from the global ensemble, while the limited-area ensemble takes its initial condition perturbations from a nine-hour forecast (to avoid any spin-up effects) from the regional ensemble providing the boundary conditions. More specifically, the limited-area ensemble is applied on a domain covering Italy and it uses three dynamical models (global, regional, local) and 14 members (the same number of the regional ensemble), a spatial grid resolution of 5.5 km (Fig. 3b) with 42 vertical levels, same number of levels of the global and the regional models. For each of the three models, different physical and dynamic schemes are used for micro-physics (Lim and Hong, 2010; Hong et al., 2004), planetary boundary layer and surface layer (Hong et al., 2006; Hong et al., 2008; Bretherton and Park, 2009; Pleim, 2006; Pleim, 2007; Beljaars, 1994), cumulus parameterization (Kain, 2004; Han and Pan, 2011), radiation (Iacono et al., 2008; Dudhia, 1989; Mlawer et al., 1997), land surface physics (Niu et al., 2011; Yang et al., 2011; Noilan and Planton, 1989; Pleim and Xiu, 1995); dynamical cores are based on the WRF-ARW (Weather Research and Forecasting-Advanced Research WRF), the WRF-NMM (Non-Hydrostatic Mesoscale Model) and the latest version of Eta model (Mesinger et al., 2012).

The 14 ensemble members at the regional scale have been chosen to reduce the large amount of computer resources required to perform the nested limited area runs for all the members of the global ensemble, making difficult to run such a system operationally. In fact, rather than using only one ensemble at the global scale, two consecutive simulations, lagged by 12 hours, are used, and they provide a set of 80 individual members. Then, an ensemble reduction technique has been applied, selecting only a few representative members of the two global time-lagged ensemble simulations in order to drive the 14-members limited-ensemble integration. The reduction procedure is carried out by performing a hierarchical cluster analysis on the EPS members (Wilks, 2006). This reduction procedure is carried out on the regional system domain, fixing the cluster number to the final number of members for the regional scale. The

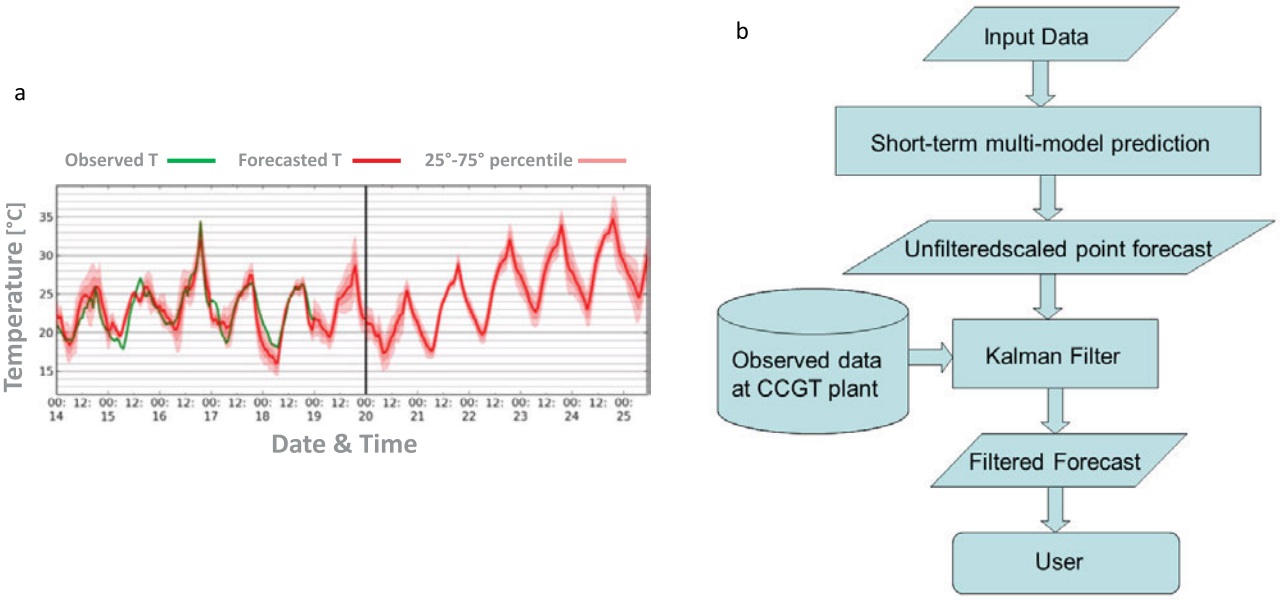

Figure 2: Observed and filtered forecast daily temperatures available for the user (a); Kalman filter application flowchart in e-kmf™ model (b).

clustering is based on the geopotential in the lower-to-middle troposphere (850, 700 and 500 hPa, respectively) at day +5 of the forecast. A representative member for each of the 14 clusters is then defined by selecting the cluster member with the minimum Euclidean distance from the other members of the same cluster and the maximum distance from all the remaining members. These 14 representatives provide initial and boundary conditions for 14 ensembles at the regional scale which, in turn, provide the initial and boundary conditions for the 14 ensembles at the limited-area domain.

The 14 individual integrations are then used to compute probabilities for the occurrence of meteorological events of interest by combining them with weights proportional to the population of the cluster they represent. Each run is post-processed through a Kalman filter in order to obtain an ensemble of temperature predictions at local scale, whose mean and spread is daily used to evaluate the power output and its variation (Fig. 2a). In this paper, only the ensemble mean is used; aware that the ensemble mean is only a minimal usage of ensemble predictions, in this specific application for power forecast, only a single hourly value of temperature can be used as input in the energy prediction system of CCGT power plants.

As weather model, the e-kmf™ forecast system is suitable for several applications where the forecast of meteorological variables is relevant, e.g. energy demand, smart grids, renewable energy, risk analysis, planning and it can be applied to any area worldwide (Giunta and Salerno, 2013).

2.2 Kalman filter application to local forecast data

It is well-known that a Kalman filter combines observations and modeled data, considering their respective error variance, for tuning the forecasted output (Persson, 1991; Kilpinen, 1992; Homleid, 1995; Galanis and Anadranistakis, 2002; Boi, 2004; Crochet, 2004; Libonati et al., 2008). The approach implemented for the e-kmf™ model is based on the non-linear correction of local forecast bias using the Kalman filter (Galanis et al., 2006), applied to post-process temperature forecasts at the CCGT power plant site by using local measured data to correct the inlet air temperature forecasts computed at the model grid scale (Fig. 2b).

In this specific work, the measurement vector (y) is defined as the difference between the locally observed (T_{obs}) and the model forecasted air temperature (T_{fct}). The observation equation is represented as polynomial function:

$$y_t = Hx_t + \varepsilon_t \tag{2.1}$$

where t is the computing time, x_t is the state vector of the polynomial coefficients updated by the Kalman filter$x = [a_0, a_1, \ldots, a_{n-1}]$, ε_t is the observation error and H is the observation vector:

$$H = [1, T_{\mathrm{fct}}, T_{\mathrm{fct}}^2, \ldots, T_{\mathrm{fct}}^{n-1}] \tag{2.2}$$

hence, the polynomial function can be explicitly written as:

$$y = a_0 + a_1 T_{\mathrm{fct}} + a_2 T_{\mathrm{fct}}^2 + \ldots + a_{n-1} T_{\mathrm{fct}}^{n-1} + \varepsilon_t \tag{2.3}$$

The state equation is defined as $x_{t+1}^t = x_t^t + \eta$ where η is the state error, which is updated with the Kalman filter as:

$$x_{t+1}^u = x_{t+1}^t + K[y - Hx_{t+1}^t - \varepsilon_t] \tag{2.4}$$

where K is the Kalman gain computed as :

$$K = PH[HPH^T + R]^{-1} \tag{2.5}$$

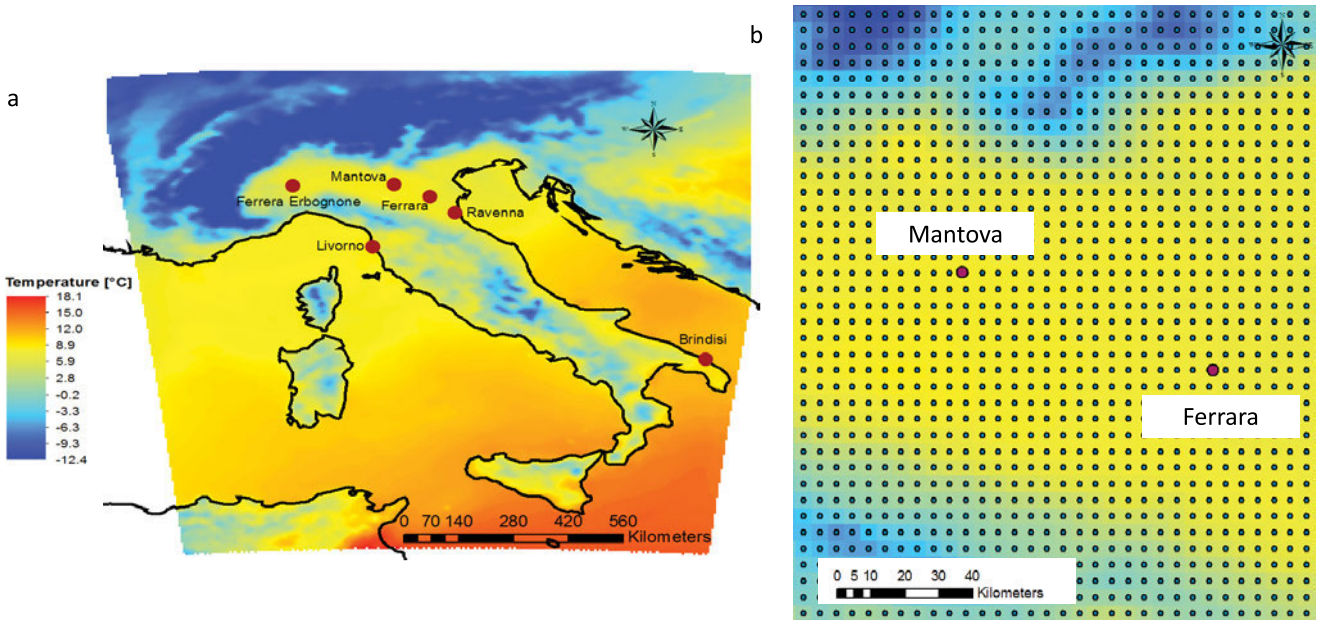

Figure 3: Map of the Italian CCGT Enipower plants (purple dots) used for carrying out the analysis for short-term temperature forecasts: the colored map shows the e-kmf™ temperature field with boundaries of the weather model domain (a), while a zoom over two plants (Mantova and Ferrara) shows the detail of the high resolution e-kmf™ grid (b).

Table 1: Bias and absolute bias of temperatures for different order of the polynomial Kalman filter and for the direct model output.

Type: Temperature [K]	Bias [K]	Absolute Bias [K]
Model output (no filter)	1.10	1.63
Degree 1 (linear)	0.25	1.39
Degree 2 (non-linear)	0.08	0.99
Degree 3 (non-linear)	−0.10	1.01
Degree 4 (non-linear)	0.12	1.05
Degree 5 (non-linear)	0.34	1.52

where R is the covariance matrix of the observation error, and P the covariance matrix of the model error (y). These last two matrixes are computed on a moving window of the previous 14 days of ε_t and η errors, whose white noise errors are Gaussian distributed.

The algorithm offers the advantage of employing non-linear functions for adjusting the difference between the grid model forecast and the local temperature values. Hereunder, a sensitivity analysis on the polynomial degree used as observation model (y) in the Kalman filter is discussed.

Different polynomial orders have been tested using a statistically significant time series, i.e. one year of hourly temperature data, to make sure that the final performance is not affected by the choice of the initial condition; these tests have been performed for several selected points in the whole Italian peninsula. Table 1 describes the performances of the observation y_t, represented by a polynomial function with a degree from 1 to 5 for hourly temperatures. Instabilities in the filter application arise quite quickly, and the performance rapidly decreases if higher polynomial degrees are used. The analysis shows that a polynomial of order 2 is the best choice for air temperatures.

2.3 Climatological features over the CCGT plant sites

The study area includes six Italian CCGT plants with 390 MW power output for each Production Unit (PU), 260 MW referred to gas turbine and 130 MW referred to steam turbine (see Fig. 3). The CCGT power plants are placed in three different climate areas: three PU are in the Po Valley, two PU in the Adriatic coast and one PU in the northern Tyrrhenian coast. The plants in the Po Valley are the most important plants, as they serve the most populated area of Italy, hence the meteorological effects may be relevant for them. It is worthwhile to remember that the Po Valley is a semi-closed basin surrounded by a very complex Alpine topography. Due to this morphology, surface winds are very weak: the average wind speed is less than 3 m/s (Giuliacci, 1988), and strong temperature inversions (in excess of 10 K) are often observed near the ground and in the boundary layer. Moreover, since the circulation in the lower troposphere is often affected by meso-scale and small-scale phenomena such as sea and mountain breeze, surface temperature inversion, and katabatic winds, like the föhn winds in the Alpine valleys, each one of the considered CCGT plant sites may be influenced by several and different phenomena, which may affect the hourly forecast of temperatures. In the Table 2, those elements, which may be not well predicted by weather models, are summarized.

Although advances in Numerical Weather Prediction (NWP) models have certainly helped to improve

Table 2: Small-scale phenomena affecting the different places where CCGT plants are located.

CCGT plant site	Katabatic winds	Fog	Thunderstorms	Sea Breezes
Ferrera Erbognone	X	X	X	
Mantova		X	X	
Ferrara		X	X	
Ravenna	X	X	X	X
Livorno			X	X
Brindisi			X	X

weather forecasts over the years, there are still limitations in predicting the exact location and intensity of these small-scale phenomena which may have a strong local influence on the CCGT plants. For meso-scale and fine-scale NWP models with grid sized ranging from 1–20 km and forecast period of 1 to 3 days, many of the resolved features, such as cumulus clouds, are not predictable and errors at these scales have sufficient time to propagate upscale (Lilly, 1983). Significant predictability may be possible for small-scale phenomena forced by the large-scale or tied to fixed forcing, such as terrain or surface heterogeneities, even if, due to uncertainties and model approximations, the depth and the space extension of the effects of such induced circulation (like in the föhn winds, for example) may be not well represented. Moreover, as in the e-kmf™ system, ensembles of very high resolution forecasts can statistically produce meaningful probabilistic forecasts. The finer orography available in such a high resolution weather prediction system gives a more accurate description of land-sea contrast (coastlines), in order to represent local phenomena such as wind over complex terrain, temperature inversions, föhn effects, drainage flow and sea breezes.

2.4 On-site observed meteorological data

Despite of all improvements of the weather models, due to the above discussed features, the local temperature predictions may still show large errors depending of the inadequate forecast of meso- and small-scale phenomena; therefore, the Kalman filter may adjust systematic errors and biases, although some are still present, due to the model limitations.

As mentioned in Section 2, temperature observations are collected on an hourly basis for each CCGT power plant in the proximity of air filter at the entrance of the gas turbine invested by the air inlet flow, and stored in a database to produce all the data used in this study. At the same time, forecasted temperature values are promptly referred to each CCGT plant site through the Kalman filter algorithm, in order to forecast local plant temperatures, which influence power production processes. This fact is important, because CCGT sites are usually located in industrial areas, where microclimates are different in comparison with the surroundings. Using the e-kmf™ model, it is possible to obtain a local and precise microclimate forecasts for these sites, and they are included in the producible electrical energy forecasting algorithm used to communicate the plant power supply at the national electric grid operator (TERNA, http://www.terna.it/en-gb/sistemaelettrico/codicedirete.aspx).

The importance of a correct prediction is controlled by a continuous feedback between forecast vs observed data with daily reports and plots. When a forecast error appears to be higher for several days, the anomaly is reported to the meteorological provider that performs a control on data flow to adjust the forecast. The possible presence of some wrong values in the observations, which may influence the Kalman filter performance, are corrected to maintain the right calibration of the forecast. At the moment, only the day before hourly data, collected each morning at 6 am CET (Central European Time), are used for the Kalman filter application.

3 Analysis of the local forecast data

Several statistical indexes have been chosen to assess this analysis in view of better describing the performance of analysed data samples. In particular, the selected indexes are the coefficient of determination (R^2), the Mean Absolute Error (MAE), the Root Mean Square Error (RMSE), the mean deviation between forecasted (Fct) and observed (Obs) data (Fct–Obs), and the Mean Relative Error (MRE), which are commonly employed in scientific literature (Wilks, 2006; Jolliffe, 2011; WWRP/WGNE Joint Working Group on Verification, http://www.cawcr.gov.au/projects/verification).

3.1 Forecasting methodology performance

The above-mentioned skill scores for each one of the six CCGT power plants are calculated both for the forecast of the following day (day+1) and for two days ahead (day+2); Fig. 4 summarizes the comparison for the e-kmf™ model between day+1 vs day+2 forecasts from 1 August 2012 to 31 August 2013. The reported results show very similar scores with a slightly better performance for day+1; however, a reliable forecast for a gas-to-power production can also be obtained two days in advance.

The e-kmf™ performance at day+1 is thoroughly investigated by calculating the percentage of cases for different forecast error ranges (i.e. temperature deviations between forecasted and observed data); average scores at given error ranges for all six CCGT plants are shown in Fig. 5 for the same analysed period (August 2012–August 2013).

By taking into account more than 50,000 cases of hourly forecasts with the e-kmf™ model, the chance of having the best forecast ($-1\,\mathrm{K} < \Delta T < 1\,\mathrm{K}$) is reasonably high, up to 40.3 %. Furthermore, analysing the e-kmf™ model sensitivity to significant air temperature variations year-round, a performance drop is detected

Ferrera Erbognone	Day + 1	Day + 2
R^2 [-]	0.93	0.92
MAE [K]	1.80	1.98
RMSE [K]	2.34	2.58
Fct-Obs [K]	0.17	0.30
MRE [-]	-0.18	0.01

Mantova	Day + 1	Day + 2
R^2 [-]	0.95	0.94
MAE [K]	1.63	1.79
RMSE [K]	2.16	2.33
Fct-Obs [K]	0.22	0.33
MRE [-]	0.03	0.10

Ferrara	Day + 1	Day + 2
R^2 [-]	0.94	0.93
MAE [K]	1.67	1.90
RMSE [K]	2.19	2.46
Fct-Obs [K]	0.10	0.21
MRE [-]	0.06	0.06

Ravenna	Day + 1	Day + 2
R^2 [-]	0.94	0.93
MAE [K]	1.74	1.85
RMSE [K]	2.31	2.44
Fct-Obs [K]	0.16	0.26
MRE [-]	0.07	0.08

Livorno	Day + 1	Day + 2
R^2 [-]	0.91	0.90
MAE [K]	1.72	1.77
RMSE [K]	2.23	2.30
Fct-Obs [K]	0.19	0.22
MRE [-]	0.03	0.03

Brindisi	Day + 1	Day + 2
R^2 [-]	0.93	0.92
MAE [K]	1.37	1.44
RMSE [K]	1.76	1.86
Fct-Obs [K]	-0.16	-0.17
MRE [-]	0.00	0.00

Figure 4: Summary of skill scores of the e-kmf™ model vs observed data for hourly temperature forecasts from 1 August 2012 to 31 August 2013 over the six CCGT power plants: the three located inland (a) and the others close to the coast (b) at day+1 and day+2 as lead time.

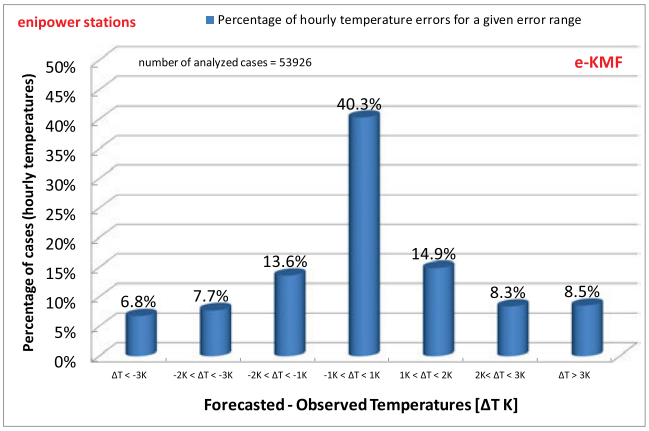

Figure 5: Percentage of cases for different forecast error ranges from 1 August 2012 to 31 August 2013 in CCGT power plants for the e-kmf™ model at day+1 as lead time.

during substantial changes in weather conditions. Since these situations can generate imbalance problems in power production, this issue is better studied in detail by calculating the percentage of errors in those events when the difference in the mean daily temperature between two consecutive days is ±4 K, which flags out a sudden change in weather conditions at synoptic scale. As shown in Fig. 6, the e-kmf™ model maintains high forecast performance in the most of the analyzed cases both for inland (Fig. 6a) and coastal (Fig. 6b) CCGT plants: the error between the forecasted and observed temperature between ±1 K (*best forecast*) is about 30.0 % out of a total of more than 3,200 analyzed cases. Hereof, better scores are found for the CCGT plants located in the proximity to the coast, where less orography is present in comparison with the ones in the Po Valley surrounded by the Alps and Apennines that can create disturbances in local forecasts. Furthermore, it is worth noting how the model forecast increases the tendency of overestimating and underestimating the observed values during these particular cases (i.e. ΔT higher than ±3 K): these latter situations are prone to generate imbalances in gas-to-power production as later described.

In fact, abrupt weather changes, variations in local conditions may have a huge impact on CCGT power generation and may generate a forecast error up to 10 K. To focus on those difficult conditions that may turn out using a weather forecast for gas-to-power production in CCGT plants, the following pictures provide some examples of special local weather situations in two CCGT sites.

For instance, an overestimation in temperature forecasts has been found during summer thunderstorms, whose episodes are not always forecasted on time by the e-kmf™ model (Fig. 7a), or during foggy days in the cold season, when forecast is a hard task at microclimate scale, and therefore the model can reach even 10 K of overestimation. Unfortunately, overestimated forecasts are not the only errors to take into account, since underestimations in temperature forecasts are present as well. In fact, an interesting consideration is highlighted in Fig. 7b for the Ferrera Erbognone power plant, where a significant deviation of temperature forecast is shown when observed temperatures range between 10 °C and 15 °C: this is mainly due to föhn (katabatic) wind episodes which are predicted with a time lag by the e-kmf™ weather model.

4 The impact of forecast temperature on power planning

Air temperature plays a relevant role in the power output of each CCGT power plant, as this latter may be significantly different from nominal power production. In fact,

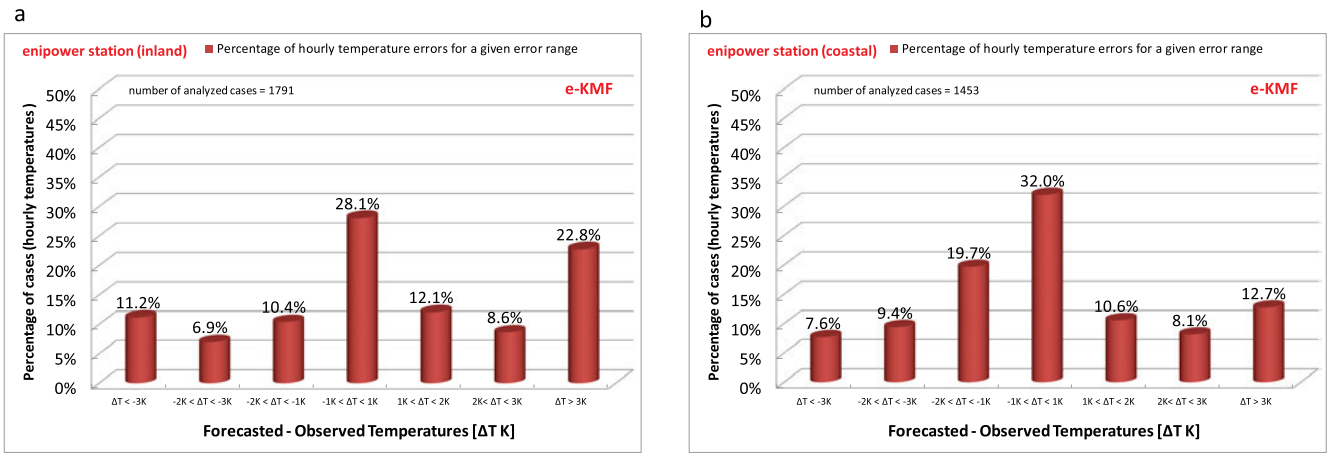

Figure 6: Percentage of cases at different forecast error ranges with the e-kmf™ model encompassing the inland (a) and coastal (b) plants at *day +1* as lead time when daily temperatures between two consecutive days are differ of more than 4 K.

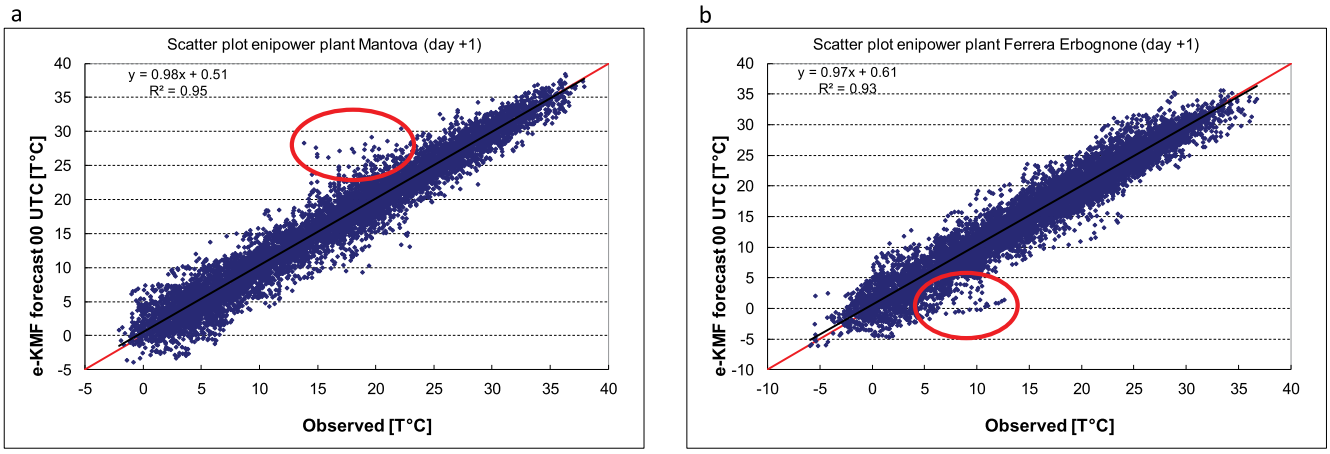

Figure 7: Scatter plots of the e-kmf™ vs observed data for the hourly temperature forecast from 1 August 2012 to 31 August 2013 for the Mantova (a) and Ferrera Erbognone (b) plants at *day+1* as lead time; the red circles highlight the significant forecast deviation vs observed values.

a Correction Factor (CF) accounts for this variation defined here below as:

$$\mathrm{CF}(T) = \text{Power output}_{\text{gross}}(T)/\text{Power output}_{nominal} \quad (4.1)$$

where: the power $\text{output}_{\text{gross}}$ is function of temperature (T) and the power $\text{output}_{\text{nominal}}$ is 390 MW for each production unit (PU).

The CF follows the two regression equations of the piecewise linear curve shown in Fig. 8. These curves have been optimized by the manufacturer of the CCGT power plant, and are valid for all Enipower fleet (same for gas and steam turbine units).

According to Fig. 8, each degree error in temperature forecasts corresponds to a variation of the available power output of about ±1.56 MW/°C for temperatures ranging between −20 °C and +15 °C and ±2.34 MW/°C for temperatures between +15 °C and +40 °C. Hence, the power output error ΔP_{out} is hereunder defined as:

$$\Delta P_{\text{out}} = Pg - Pp \quad (4.2)$$

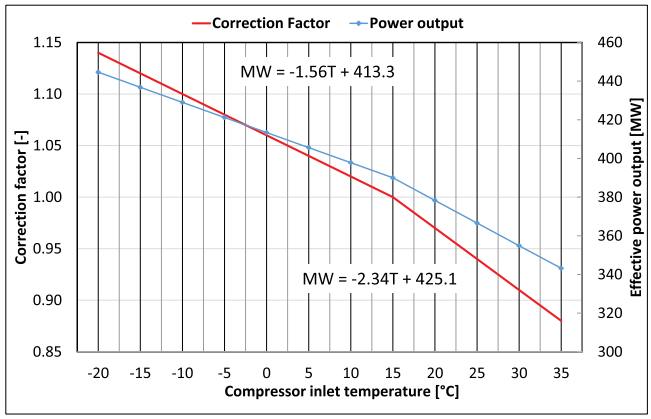

Figure 8: Relationship between correction factor (in red) and power output (in blue) in CCGT power plants. T, shown in the two equations above, stands for the observed/forecasted temperature.

where Pg is the generated gross power and Pp is the programmed power output (in MW), both computed assuming observed (T_{obs}) and forecasted (T_{fct}) temperature, respectively (Fig. 9).

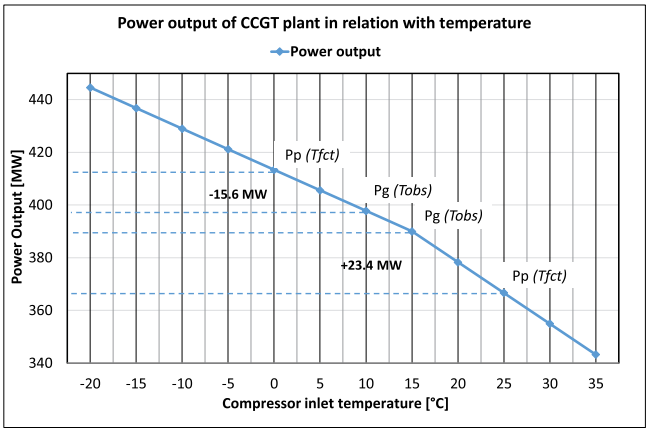

Figure 9: Relationship between power output (in MW) and observed/forecasted temperatures at the air intake of the gas turbine.

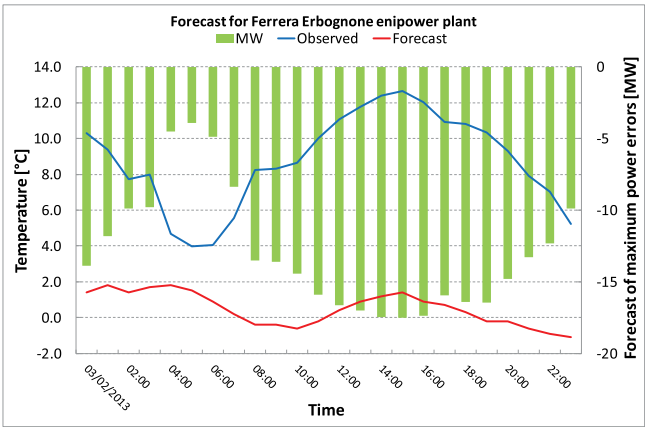

Figure 10: Temperature forecasts (red line) issued on 02 February 2013 valid for the following day compared with observed data (blue line); negative forecast power errors ΔP_{out} in MW are plotted in green bars.

A temperature forecast error of ±10 °C in one hour can generate up to ±15 MW or ±23 MW of potential power deviations for any production unit (PU), if observed temperatures are below or over 15 °C, respectively.

This power error ΔP_{out} is the driving variable which quantifies the role of meteorological forecasts on CCGT power plants. In particular, negative errors between T_{obs} and T_{fct} due to underestimations of temperature forecasts produce differences in the power output by the CCGT plant, which cause operative charges due to the electric grid imbalance. On the contrary, errors due to an overestimation of the T_{fct} determine an unsold power output that is less onerous than the previous one. These electric grid imbalance charges between produced and programmed electricity by each power plant in Italy are metered by TERNA in accordance with the national grid code. Parenthetic clause, the Italian electric grid operator (TERNA) performs every day the services of electrical energy transport along the national transmission grid, and the services of dispatching, by maintaining the balance between the input and withdrawal of electrical energy with the necessary reserve margins.

For instance, considering a forecasting local temperatures error for the following day over the Ferrera Erbognone CCGT power plant during a winter day in February 2013, as shown in Fig. 10, a daily average deviation of about 8 K and peaks up to 11 K between forecasted and observed data can generate an imbalance in power output up to 310 MW as total in 24 hours, due to a wrong forecast of a föhn episode, not predicted by the meteorological model in the southern edge of the Alps.

Thus, to estimate positive and negative cumulated errors in the whole thirteen analyzed months in 2012 and 2013, the effective power output (in MW) is here computed for two CCGT plants, Brindisi and Ferrera Erbognone (Fig. 11), which are under different climate conditions. In particular, for the Brindisi CCGT power plant (Fig. 11a), significant power errors are observable during intermediate seasons (autumn 2012 and spring 2013), while lower values are recorded in the winter season 2012–2013. In this period, the Adriatic Sea is exposed to the influence of cyclones with the northeaster Bora and the southeastern (SE) winds. Northeastern (NE) winds are a cold flux common in the winter season. It blows at intervals from the NE direction, and it is stronger along the coast, and weaker towards the open sea. This typical situation reduces the differences between maximum and minimum temperatures and, hence, it reduces the variation between observed and forecasted temperatures.

On the contrary, for Ferrera Erbognone plant (Fig. 11b), higher power deviations are highlighted between May and September 2013, when a greater weather variability affected the Po Valley area, vis-à-vis colder months (from October 2012 to April 2013) are characterized by more events of stable conditions, although some occasional föhn winds (katabatic), as in the example above-described, can generate high daily negative imbalances.

5 Conclusions

Nowadays, meteorological models are largely used for several applications in different fields both for forecasts of public interests as well as for economic issues. The paper describes how the application of a high-resolution limited area model, the eni-Kassandra Meteo Forecast model (e-kmf™), developed by Eni S.p.A, and a Kalman filter to post-process model output data can predict accurate hourly temperature. These data are operatively used to daily optimize the gas-to-power generation process in CCGT power plants and to reduce the penalties concerning imbalance charges on the national power grid operated by TERNA. The analysis has covered a period of thirteen months (1 August 2012–31 August 2013). The main results highlight a high level of performance with no significant differences between day+1 and the day+2 forecasts (MAE equal to 1.66 K and 1.79 K, respectively), so that energy planning can be programmed with the day +2 forecast, as well.

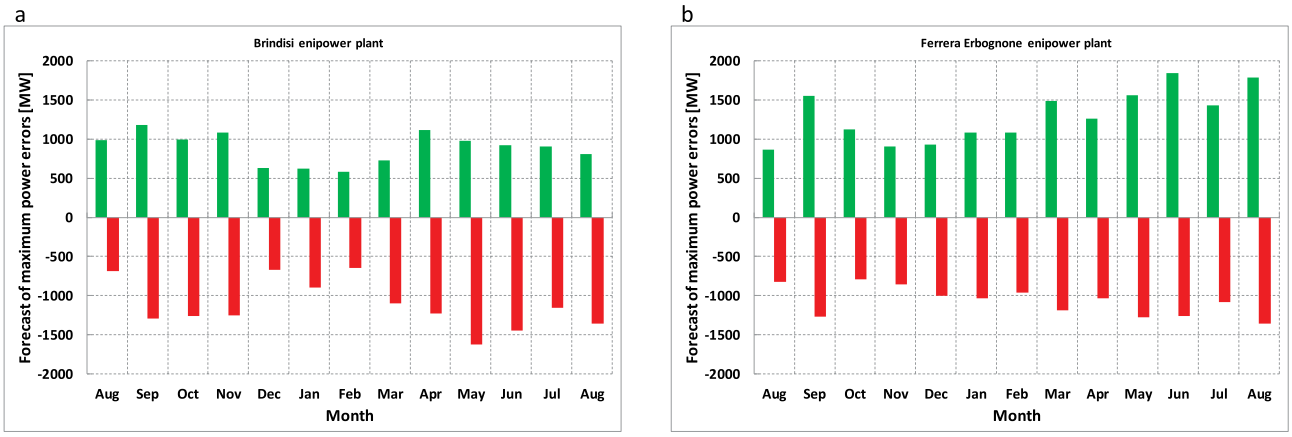

Figure 11: Forecasting power output errors ΔE_{out} (positive in green columns and negative in red columns) for the two CCGT plants (Brindisi, (a) and Ferrera Erbognone, (b)) from August 2012 to August 2013.

Some limitations in the present application have been also evidenced by analysing short-term temperature forecasts concerning six Italian CCGT power plants (Mantova, Brindisi, Ferrara, Ravenna, Livorno, and Ferrera Erbognone). In particular, some flaws in the e-kmf™ model performance were detected during some local scale phenomena such as summer thunderstorms, winter fogs and secondary orography-induced circulation. These phenomena must be taken into account when weather forecasts are used at local scale to estimate the producible electric power.

In fact, during significant weather change conditions (temperature differences are ±4 K between two days in advance), the chance of having the *best forecast* (±1 K between forecasted and observed) decreases from 40.3 % down to about 30.0 %, while the percentage of having over/underestimation of ±3 K increases, in particular for inland CCGT plant sites. These deviations can contribute to positive and negative errors in power output generation in each plant.

Some weather scenarios are not correctly identified by the model and the forecast performances are reduced. These faults might be mitigated by connecting local measurements to the forecast system, by a frequently updating, instead of the day-before data only, improving the Kalman filter gain and reducing the estimation errors of the post-processing. This methodology will be investigated in the near future, in order to finalize an operative application for all CCGT power plants.

List of abbreviations used

CCGT: Combined-Cycle Gas Turbine
CET (Central European Time)
CHP: Combined heat and power
e-kmf™: eni-kassandra meteo forecast
EMF: Ensemble Mean Forecast
ETKF: Ensemble Transform Kalman Filter
GT: Gas Turbine
LAM: Limited Area Model
MAE: Mean Absolute Error
ME: Mean Error
MRE: Mean Relative Error
NWP: Numerical Weather Prediction
PDF: Probability Density Function
PU: Production Unit
RMSE: Root Mean Square Error
WRF-NMM: Weather Research Forecast – Non-Hydrostatic Mesoscale Model
WRF-ARW: Advanced Research WRF

Acknowledgments

This research was carried out in the framework of the Kassandra Meteo project founded by Eni S.p.A. The authors thank Dr. C. Corbari for her help in reviewing the Kalman filter analysis.

References

Beljaars, A.C.M., 1994: The parameterization of surface fluxes in large-scale models under free convection. – Quart. J. Roy. Meteor. Soc.**121**, 255–270.

Bishop, C.H., B.J. Etherton, S.J. Majumdar, 2001: Adaptive sampling with the ensemble transform Kalman Filter. Part I: Theoretical aspects. – Mon. Wea. Rev. **129**, 420–435.

Boi, P., 2004: A statistical method for forecasting extreme daily temperatures using ECMWF 2-m temperatures and ground station measurements. – Meteorol. Appl. **11**, 245–251.

Boonnasa, S., 2006: Performance improvement of the Combined Cycle Power Plant by intake air cooling using an absorption chiller. – Energy **31**, 2036–2046.

Bretherton, C.S., S. Park, 2009: A new moist turbulence parameterization in the Community Atmosphere Model. – J. Climate **22**, 3422–3448.

Crisostomi, E., A. Franco, G. Giunta, M. Raugi, 2013: The Smart Gas Grid: state of the art and perspectives. – IEEE PES Innovative Smart Grid Technologies Europe (ISGT Europe), Copenhagen.

Crochet, P., 2004: Adaptive Kalman filtering of 2-metre temperature and 10-metre wind-speed forecasts in Iceland. – Meteorol. Appl. **11**,173–187.

De Felice, M., A. Alessandri, F. Catalano, 2015: Seasonal climate forecasts for medium-term electricity demand forecasting. – Appl. Energy **137**, 435–444.

Dudhia, J., 1989: Numerical study of convection observed during the Winter Monsoon Experiment using a mesoscale two-dimensional model. – J. Atmos. Sci. **46**, 3077–3107.

Farouk, N., L. Sheng, Q. Hayat, 2013: Effect of ambient temperature on the performance of gas turbines power plant. – Int. J. Comp. Sci. **10**, 439–442.

Galanis, G., M. Anadranistakis, 2002: A one-dimensional Kalman filter for the correction of near surface temperature forecasts. – Meteorol. Appl. **9**, 437–441.

Galanis, G., P. Louka, P. Katsafados, I. Pytharoulis, G. Kallos, 2006: Applications of Kalman filters based on non-linear functions to numerical weather predictions. – Ann. Geophys. **24**, 2451–2460. DOI:10.5194/angeo-24-2451-2006.

Gareta, R., L.M. Romeo, A. Gil, 2004: Methodology for the economic evaluation of gas turbine air cooling systems in combined cycle applications. – Energy **29**, 1805–1818.

Giuliacci, M., 1988: Climatologia fisica e dinamica della Valpadana [in Italian]. ERSA, Bologna.

Giunta, G., R. Salerno, 2013: Short-long term temperature forecasting method and system for production management and sale of energy resources. – WO Patent App. PCT/IB2013/0546780, WO 2013/186703 A1.

Giunta, G., R. Salerno, A. Ceppi, G. Ercolani, M. Mancini, 2015: Benchmark analysis of forecasted seasonal temperature over different climatic areas. – Geosci. Lett. **2**, 9. DOI: 10.1186/s40562-015-0026-z.

Han, J., H.-L. Pan, 2011: Revision of convection and vertical diffusion schemes in the NCEP Global Forecast System. – Wea. Forecasting **26**, 520–533. DOI:10.1175/WAF-D-10-05038.1.

Homleid, M., 1995: Diurnal corrections of short-term surface temperature forecasts using the Kalman filter. – Wea. Forecasting **10**, 689–707.

Hong, S.-Y., J. Dudhia, S.-H. Chen, 2004: A revised approach to ice microphysical processes for the bulk parameterization of clouds and precipitation. – Mon. Wea Rev. **132**, 103–120.

Hong, S.-Y., Y. Noh, J. Dudhia, 2006: A new vertical diffusion package with an explicit treatment of entrainment processes. – Mon. Wea. Rev. **134**, 2318–2341.

Hong, S.-Y., J. Choi, E.-C. Chang, H. Park, Y.-J. Kim, 2008: Lower-tropospheric enhancement of gravity wave drag in a global spectral atmospheric forecast model. – Wea. Forecasting **23**, 523–531. DOI:10.1175/2007WAF2007030.1.

Iacono, M.J., J.S. Delamere, E.J. Mlawer, M.W. Shephard, S.A. Clough, W.D. Collins, 2008: Radiative forcing by long–lived greenhouse gases: Calculations with the AER radiative transfer models. – J. Geophys. Res. **113**, D13103. DOI: 10.1029/2008JD009944.

Jolliffe, I.T., D.B. Stephenson, 2011: Forecast verification: a practitioner's guide in atmospheric science. – Wiley, New York, 292 pp.

Kain, J.S., 2004: The Kain–Fritsch convective parameterization: An update. – J. Appl. Meteor. **43**, 170–181.

Kakaras, E., A. Doukelis, A. Prelipceneau, S. Karellas, 2005: Inlet air cooling methods for gas turbine based power plants. – J. Eng. Gas Turbines Power **128**, 312–317.

Kehlhofer, R., B. Rukes, F. Hannemann, F. Stirnimann, 2009: Combined-Cycle Gas & Steam Turbine Power Plants. – PennWell Books, 430 pp.

Kilpinen, J., 1992: The application of Kalman filter in statistical interpretation of numerical weather forecast. – Proc. 12th Conf. on Probability and Statistics in Atmospheric Sciences, Toronto, Canada. Amer. Meteor. Soc., 11–16.

Libonati, R., I. Trigo, C.C. Dacamara, 2008: Correction of 2 m-temperature forecasts using Kalman Filtering technique. – Atmos. Res. **87**, 183–197.

Lilly, D., 1983: Stratified turbulence and the mesoscale variability of the atmosphere. – J. Atmos. Sci. **40**, 749–761.

Lim, K.-S., S.-Y. Hong, 2010: Development of an effective double–moment cloud microphysics scheme with prognostic cloud condensation nuclei (CCN) for weather and climate models. – Mon. Wea. Rev. **138**, 1587–1612.

Lorenz, E.N., 1963: Deterministic nonperiodic flow. – J. Atmos. Sci. **20**, 130–141.

Lorenz, E.N., 1965: A study of the predictability of a 28-variable atmospheric model. – Tellus **17**, 321–333.

Lorenz, E.N., 1982: Atmospheric predictability experiments with a large numerical model. – Tellus **34**, 505–513.

Mass, C.F., D. Ovens, K. Westrick, B.A. Colle, 2002: Does increasing horizontal resolution produce more skillful forecasts? – Bull. Amer. Meteor. Soc. **83**, 407–430.

Mesinger, F., S.C. Chou, J.L. Gomes, D. Jovic, P. Bastos, J.F. Bustamante, L. Lazic, A.A. Lyram, S. Morelli, I. Ristic, K. Veljovic, 2012: An Upgraded Version of the Eta Model. – Meteor. Atmos. Phys. **116**, 63–79.

Mlawer, E.J., S.J. Taubman, P.D. Brown, M.J. Iacono, S.A. Clough, 1997: Radiative transfer for inhomogeneous atmospheres: RRTM, a validated correlated-k model for the longwave. – J. Geophys. Res. **102**, 16663–16682.

Niu, G.-Y., Z.-L. Yang, K.E. Mitchell, F. Chen, M.B. Ek, M. Barlage, A. Kumar, K. Manning, D. Niyogi, E. Rosero, M. Tewari, Y. Xia, 2011: The community Noah land surface model with multiparameterization options (Noah–MP): 1. Model description and evaluation with local-scale measurements. – J. Geophys. Res. **116**, D12109.

Noilan, J., S. Planton, 1989: A simple parameterization of land surface processes for meteorological models. – Mon. Wea. Rev. **117**, 536–549.

Persson, A., 1991: Kalman filtering a new approach to adaptive statistical interpretation of numerical meteorological forecasts. Lectures and papers presented at the WMO Training Workshop on the Interpretation of NWP Products in Terms of Local Weather Phenomena and Their Verification, Wageningen, the Netherlands, WMO TD 421, pp. XX.

Pleim, J.E., 2006: A Simple, efficient solution of flux-profile relationships in the atmospheric surface layer. – J. Appl. Meteor. Climatol. **45**, 341–347.

Pleim, J.E., 2007: A Combined Local and Nonlocal Closure Model for the Atmospheric Boundary Layer. Part I: Model Description and Testing. – J. Appl. Meteor. Climatol. **46**, 1383–1395.

Pleim, J.E., A. Xiu, 1995: Development and testing of a surface flux and planetary boundary layer model for application in mesoscale models. – J. Appl. Meteor. **34**, 16–32.

Rovira A., C. Sanches, M. Munoz, M. Valdes, M.D. Duran, 2011: Thermoeconomic optimisation of heat recovery steam generators of combined cycle gas turbine power plants considering off-design operation. – Energy Conversion and Management **52**, 1840–1849.

Toth, Z., Y. Zhu, T. Marchok, 2001: The ability of ensembles to distinguish between forecasts with small and large uncertainty. – Wea. Forecasting **16**, 436–477.

Wilks, D.S., 2006: Statistical methods in the atmospheric sciences. – Academic Press, New York, 704 pp.

Yang, Z.-L., G.-Y. Niu, K.E. Mitchell, F. Chen, M.B. Ek, M. Barlage, L. Longuevergne, K. Manning, D. Niyogi, M. Tewari, Y. Xia, 2011: The community Noah land surface model with multiparameterization options (Noah–MP): 2. Evaluation over global river basins. – J. Geophys. Res. **116**, D12110.

Zadpoor, A.A., A.H. Golshan, 2006: Performance improvement of a gas turbine cycle by using a desiccant-based evaporative cooling system. – Energy **31**, 2652–2664.